



Flare-Shaped Acoustic Anomalies in the Water Column Along the Ecuadorian Margin: Relationship with Active Tectonics and Gas Hydrates

FRANCOIS MICHAUD,^{1,2} JEAN-NOËL PROUST,³ ALEXANDRE DANO,² JEAN-YVES COLLOT,^{2,4} GRÂCE DANIELLA GUIYELIGOU,² MARÍA JOSÉ HERNÁNDEZ SALAZAR,⁵ GUEORGUI RATZOV,² CARLOS MARTILLO,^{2,3,6,7} HUGO POUDEIROUX,³ LAURE SCHENINI,² JEAN-FREDERIC LEBRUN,⁸ and GLENDA LOAYZA^{6,7}

Abstract—With hull-mounted multibeam echosounder data, we report for the first time along the active Ecuadorian margin, acoustic signatures of water column fluid emissions and seep-related structures on the seafloor. In total 17 flare-shaped acoustic anomalies were detected from the upper slope (1250 m) to the shelf break (140 m). Nearly half of the flare-shaped acoustic anomalies rise 200–500 m above the seafloor. The base of the flares is generally associated with high-reflectivity backscatter patches contrasting with the neighboring seafloor. We interpret these flares as caused by fluid escape in the water column, most likely gases. High-resolution seismic profiles show that most flares occur close to the surface expression of active faults, deformed areas, slope instabilities or diapiric structures. In two areas tectonic deformation disrupts a Bottom Simulating Reflector (BSR), suggesting that buried frozen gas hydrates are destabilized, thus supplying free gas emissions and related flares. This discovery is important as it opens the way to determine the nature and origin of the emitted fluids and their potential link with the hydrocarbon system of the forearc basins along the Ecuadorian margin.

Key words: Ecuador, Subduction, Continental margin, Multibeam, Backscatter, Fluid, Seepage, Acoustics.

1. Introduction

In the past decade, the increase in multibeam seabed and water column mapping shows that seepage activity at continental margins is a relatively widespread phenomena (LONCKE *et al.* 2004; DUPRÉ *et al.* 2010; 2014; MASCLE *et al.* 2014). In seafloor seepage activity areas, vents are detected by images of plumes in the water column (MEREWETHER *et al.* 1985; HORNAFIUS *et al.* 1999; GERMAN *et al.* 1996; GREINERT *et al.* 2006; DUPRÉ *et al.* 2010). The basic principle for detecting plumes with echo sounders is the high backscattering of the pressure wave at the impedance contrasts between water and gas bubbles (SCHNEIDER VON DEIMLING *et al.* 2007). This creates flare-shaped backscatter features in echograms. Most acoustic anomalies recorded in the water column with multibeam echo sounders are caused by fluid escape at the seabed, most likely gases (JUDD and HOVLAND 2007).

Along continental margins, submarine cold seeps are sites where fluids, either pore water or free gas, migrate upward from buried sedimentary horizons. They are also often inferred to be associated with gas hydrates in the underlying sediment, which can act as sources for methane, the dominant gas component at most seeps (KRABBENHÖFT *et al.* 2010; RÖMER *et al.* 2014). Hydrates are evidenced and mapped based on the distribution of Bottom Simulating Reflector (BSR), a characteristic seismic reflection caused by

¹ Univ. Pierre et Marie Curie, UPMC, CNRS, IRD, Observatoire de la Côte d'Azur, Géoazur UMR 7329, 250 rue Albert Einstein, 06560 Sophia Antipolis, Valbonne, France. E-mail: micho@geoazur.unice.fr

² Univ. Nice Sophia Antipolis, CNRS, IRD, Observatoire de la Côte d'Azur, Géoazur UMR 7329, 250 rue Albert Einstein, 06560 Sophia Antipolis, Valbonne, France.

³ Géosciences Rennes, CNRS, Université de Rennes 1, Campus de Beaulieu, 35042 Rennes Cedex, France.

⁴ Investigador Prometeo, Instituto Geofísico, Escuela Politécnica Nacional, Ladrón de Guevara E11-253, Aptdo.2759 Quito, Ecuador.

⁵ Departamento de Geología, Escuela Politécnica Nacional, Ladrón de Guevara E11-53, Quito, Ecuador.

⁶ Facultad de Ingeniería en Ciencias de la Tierra, Escuela Politécnica del Litoral, km 30.5 Vía Perimetral Campus "Gustavo Galindo", Guayaquil, Ecuador.

⁷ Instituto Oceanográfica de la Armada de Ecuador (INOCAR), Avenida 25 de Julio vía Puerto Marítimo, Base Naval Sur, Guayaquil, Ecuador.

⁸ Univ. des Antilles et de la Guyane, Campus de Fouillole, 97159 Pointe a' Pitre Cedex, Guadeloupe, France.

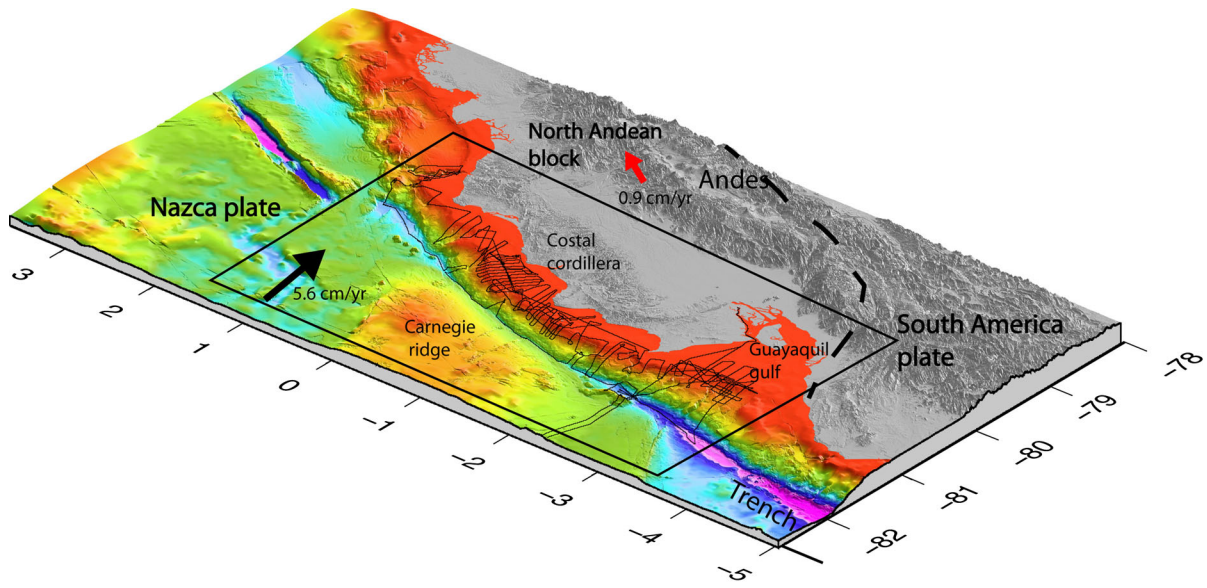


Figure 1

Geodynamic framework of the study area. The Nazca plate subducts beneath the South American continent at velocity of 5.6 cm/year (NOCQUET *et al.* 2009) and the North Andean block move to the North at a velocity of 0.9 cm/year (NOCQUET *et al.* 2014). The forearc area is characterized by the arrival in the trench of the Carnegie Ridge and the escape to the North of the North Andean block. Location of the Fig. 2 (box). Thick black dashed line = eastern boundary of the North Andean block from BOURGOIS (2013). Thin black lines = ATACAMES shiptracks

the strong impedance contrast between hydrate-containing sediment above and gas-filled pore space below.

Seafloor fluid flow occurs in a wide range of oceanographic environments and geological contexts (JUDD and HOVLAND 2007). Seepage may be associated with undercompaction sediments (JUDD and HOVLAND 2007), slope instabilities (PAULL *et al.* 1998; PRAEG *et al.* 2014) and seafloor deformation (DEYNOUX *et al.* 1990; DANO *et al.* 2014). Some seeps are associated with active faulting (GAY *et al.* 2007; GELI *et al.* 2008; DUPRÉ *et al.* 2015) with release of fluids along the faults. Such tectonically driven mechanism could feed hydrate-related vents and associated seepage (SUESS *et al.* 1999). Consequently, in many cases the detection of flare in the water column indicates active tectonic structure, or slope instabilities.

This paper provides a first, non-exhaustive, account of water-column acoustic flares along the active Ecuadorian margin and a discussion on the potential first-order relationships with tectonics and sedimentary features. This fluid system was

discovered by multibeam bathymetric data acquired in 2012 during the ATACAMES campaign (MICHAUD *et al.* 2013) conducted on the R/V *L'Atalante* (IFREMER).

2. Geological Setting

Along the Ecuadorian margin, the Nazca plate (Fig. 1) subducts eastwards at a 5.6 cm year⁻¹ rate beneath the South America plate (NOCQUET *et al.* 2014). The evolution of the Ecuador margin is strongly influenced by the subduction of the Carnegie Ridge (MICHAUD *et al.* 2009; COLLOT *et al.* 2009) and the northward tectonic escape of the North Andean block at a 0.95 cm year⁻¹ rate (NOCQUET *et al.* 2014) (Fig. 1). In the forearc, sediment supply from the Andes is deflected northwards and southwards by the uplift of the coastal cordillera (COLLOT *et al.* 2009). The uplift of the coastline and coastal range appears to have related to the subduction of the Carnegie Ridge (PEDOJA *et al.* 2006; GUTSCHER *et al.* 1999; PROUST *et al.* 2016) for, at least, the last 1.3 Ma

(GRAINDORGE *et al.* 2004) or 4–5 Ma (COLLOT *et al.* 2009). The subduction of the Carnegie Ridge is synchronous with the acceleration of the North Andean block escape (WITT *et al.* 2006) and an increase of the subsidence rate in the Gulf of Guayaquil (DENIAUD *et al.* 1999) since the Early Pleistocene.

The usually smooth and linear continental margin slope becomes irregular south of 1°35'S (COLLOT *et al.* 2009), where the margin faces the incoming Carnegie Ridge. Several 1–2 km high, 10–15 km large subducting seamounts indent locally the lower margin slope (Fig. 2), (SAGE *et al.* 2006; MARCAILLOU *et al.* 2016). As shown along other convergent margins, morphologic embayment-related subducted-seamounts result from slope material removal by tunneling of underthrusting seamounts (DOMINGUEZ *et al.* 1998; RANERO and VON HUENE 2000; MARCAILLOU *et al.* 2016).

Several main regional faults deform the margin seafloor. In the North of Ecuador, the trench sub-parallel Ancon fault that is locally associated with a crustal splay fault deforms sediments along the trench slope break (COLLOT *et al.* 2004, 2005, 2008); the onshore Galera fault system (EGUEZ *et al.* 2003) may extend seaward oblique to the shelf break and upper margin slope (MICHAUD *et al.* 2015), and, in Central Ecuador, the oblique to the margin Jama fault system extends offshore along a small upper slope sedimentary basin and is interpreted as a negative flower structure (Fig. 2), (COLLOT *et al.* 2004; MICHAUD *et al.* 2015).

Bottom Simulating Reflectors (BSR) are widely extended along the southern Colombian margin (MARCAILLOU *et al.* 2006). Along the Ecuadorian margin, multichannel seismic lines shot in the Ancon fault area (MARCAILLOU *et al.* 2006) (Fig. 2) show a BSR; and southward, until 0°00'N of latitude, BSR is also reported along the slope (MARCAILLOU *et al.* 2016).

3. Methods

Multibeam data were acquired using a hull-mounted Simrad EM710 and EM122 multibeam echosounder, yielding a Digital Terrain Models with a resolution of 25 m for bathymetry and 10 m for

backscatter imagery. The data were processed using the seafloor mapping software CARAIBES (developed by IFREMER). Water column data were acquired along selected swaths, processed and visualized using Sonarscope software (developed by IFREMER). Sub-bottom profiles were acquired with a hull-mounted Chirp system (1.8–5.3 kHz). Seismic reflection data were recorded using a 72-channel digital streamer towed at 2 m of water depth (channel length 6.25 m). The source array towed at 2.1 m of water depth consisted of two ramps mounted with three 13/13 cubic-inch plus three 24/24 cubic-inch mini GIGun. Shots were fired at 140 bars every 25 m. Given the shot rate and the streamer configuration, this seismic reflection system ensures a ninefold stack. The seismic lines were processed onboard with the Seismic Unix (SU) software (Center of Wave Phenomena, Colorado School of Mines) for Band Pass Filtering, spherical divergence correction (water velocity)—NMO velocity analysis and correction, ninefold stack and constant velocity time migration (1490 m/s).

4. Results

We detected 17 plume sites along the Ecuadorian margin (Table 1, black dots in Fig. 2). The seeps concentrate in four main areas (Fig. 2). Two sites are located near the shelf break (site 3 and 15) whilst all others are seated on the upper slope, ranging from 140 to 1250 m in water depth.

To the north (Esmeraldas canyon area, Fig. 3) three plume sites were discovered on the western side of the Esmeraldas canyon. Sites 1 and 2 are very close together (3 km apart) and located around 1100–1200 m of water depth. The most spectacular is the 500 m high plume at site 1 (Fig. 3b). The seafloor backscatter image shows that plume sites 1 and 2 correspond to ~100 m large high-reflectivity sub-circular patches (Fig. 3c). Site 3 is located near the shelf break, just on the edge of a 5-km wide semi-circular slope re-entrant with irregular rim; this re-entrant does not breach the shelf break. The NS seismic profile shot across site 1 (Fig. 3d) shows deformed strata and lateral seismic facies changes. Plume site 1 locates above a transparent seismic

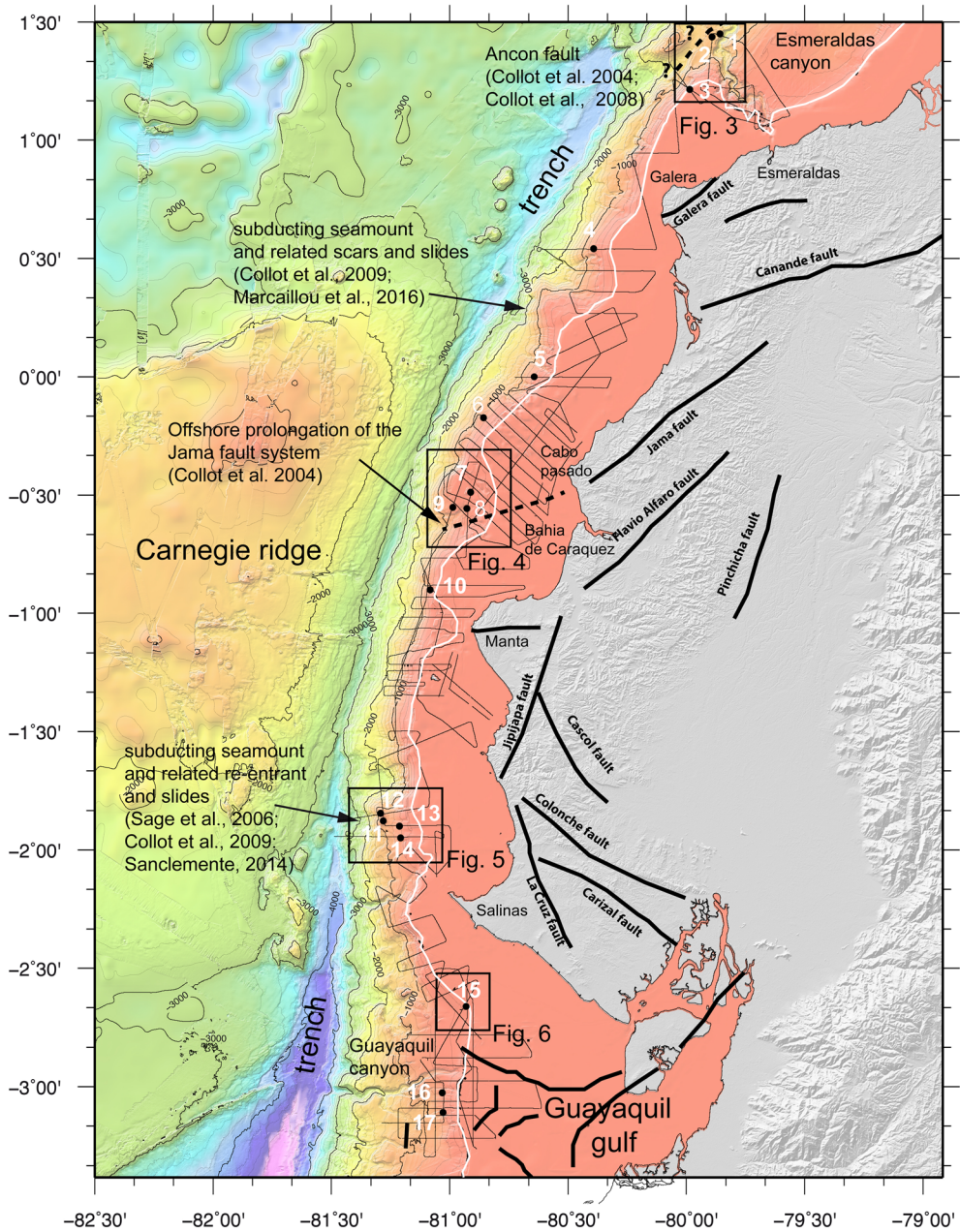


Figure 2

Bathymetric map (black circles with number = location of plume sites detected in this work). Thick black lines = principal faults on land from REYES and MICHAUD (2012); Offshore faults in the Gulf of Guayaquil are from WITT *et al.* (2006). Thick dotted black line = prolongation offshore of the Jama fault system inferred by COLLOT *et al.* (2004). Fine white line = 150 m isobath. Fine black lines = location of seismic profiles recorded during the ATACAMES cruise (MICHAUD *et al.* 2013).

facies, which underlines a diapir structure more and less rooted in a BSR. Southward of the diapir, the most recent sediments show important change of seismic facies from chaotic (b on Fig. 3d), to sub

parallel reflector facies dipping to the south (a on Fig. D) and to the north (c on Fig. D). This sediment fill is bounded to the South by a faulted monocline (Fig. 3d).

Table 1

Location and main characteristics of acoustic anomalies

Acoustic anomaly	Latitude (°)	Longitude (°)	Depth in meter	Plumes high in meter	Areas
1	1.4367	-79.8915	1225	500	Esmeraldas canyon area
2	1.4501	-79.8589	1100	300	
3	1.2153	-79.986	140	50	
4	0.5425	-80.3932	630	>100	Isolated anomaly on the upper slope
5	-0.1733	-80.8577	600	>100	
6	-0.001	-80.6443	675	150	Offshore prolongation of the Jama fault system area
7	-0.5567	-80.928	475	100	
8	-0.4885	-80.9118	575	>100	
9	-0.5522	-80.988	612	220	
10	-0.9006	-81.0826	600	>100	
11	-1.8406	-81.1973	790	300	Subducting seamount area
12	-1.8449	-81.2923	700	250	
13	-1.8769	-81.2817	660	300	Gulf of Guayaquil area
14	-1.8994	-81.2131	650	300	
15	-2.6609	-80.931	160	100	
16	-3.0264	-81.0317	550	150	
17	-3.1092	-81.0287	560	350	

Plume sites 4, 5, and 6 (Fig. 2) are isolated along ship tracks. They are located on the upper slope between 600 and 675 m of water depth (Table 1). They are more and less 100 m high. On the seismic profiles crossing these plume areas, sub-vertical acoustic anomalies are present and could be indicative of fluids flows from bottom levels. But the seismic profiles do not show any related specific tectonic or slope failure structures.

The offshore prolongation of the Jama fault system area (Fig. 4) shows three plume sites 7, 8, and 9, located at a water depth of about 500 m (Table 1; Figs. 2 and 4a). Plume 9 is about 200 m high (Fig. 4b) when plumes 7 and 8 are 100 m high (Fig. 4b). Plume sites 7 and 8 are located in a deformed sedimentary basin (unit c on Fig. 4c). Plume site 7 is detected in an area of the basin affected by sub vertical faults. Plume 8 is associated with a diapir expressed on the seafloor by a sub-circular, 15 m high and 500 m wide feature (Fig. 4d). Plume site 9 is located at the southern edge of this basin (Fig. 4e, d). At the site 9, unconformities are observed on the seismic profile (Fig. 4e); a chaotic unit (a on Fig. 4e) is topped by a unit with NE-inclined parallel reflectors (b on Fig. 4e). At this place the slope is affected by a semi-circular 2 km wide re-entrant oriented in a seaward direction that breaches a 100 m high linear scarp (Fig. 4d).

Plume site 10 (Table 1; Fig. 2) is isolated on the upper slope. The plume is less than 150 m high and is poorly developed in the water column.

Plume sites 11, 12, 13, and 14 (Table 1; Fig. 2) are grouped in an area that is approximately 20 km long ranging between 800 and 600 m of water depth. Each site shows a ~300 m high flare. Plume sites 11 and 12 are located on the NS-trending crest of a 100-m bathymetric high (Fig. 5) on the slope between 600 and 1000 m of water depth. The seismic profile shows that this high is highly deformed (Fig. 5d) flanked by a continuous BSR partially disrupted at the top of the ridge. The seafloor backscatter image shows that plume sites 11 and 12 correspond to ~100 m sub-circular high-reflectivity patches (Fig. 5c). Plume sites 13 and 14 are located higher on the slope bathed in 650 m of water depth but the seismic profiles do not show clear related structure.

Plume site 15 is located at the shelf break of the gulf of Guayaquil (Table 1; Figs. 2 and 6a). This site is remarkable because it exhibits several plumes (Fig. 6b). This site is in the center of a rough seafloor morphology (Fig. 6a and e) that defines an irregular 2 km large and 20 m high dome above the surrounding seafloor. The seafloor backscatter image (Fig. 6c) shows that this dome is associated with a set of high-reflectivity backscatter patches; the plume is at the center of an ellipsoid-shaped low-reflectivity patch. In

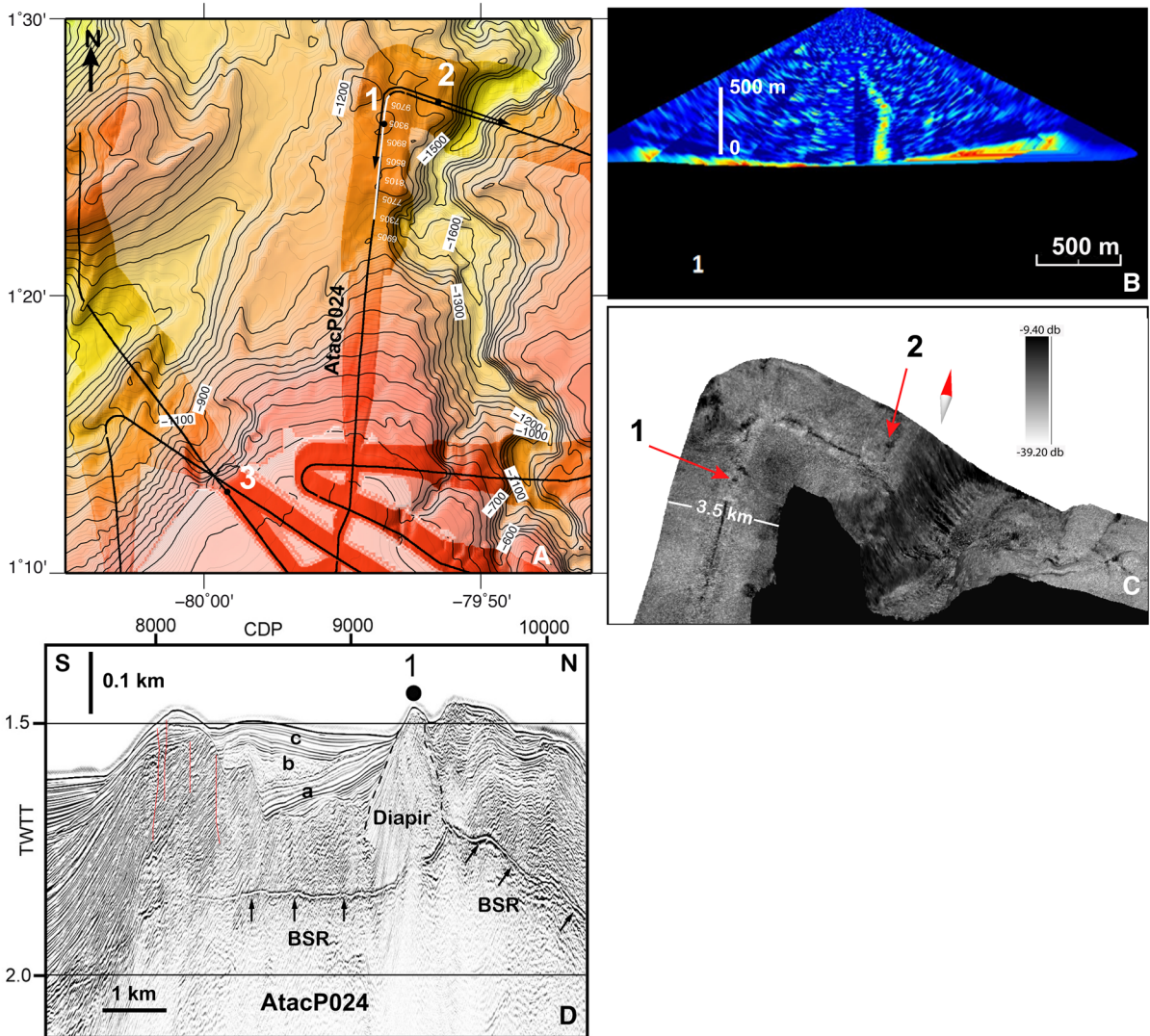


Figure 3

a Bathymetric map with curves every 20 m (location on Fig. 2) of the Canyon Esmeraldas area (grid cell 50 m). More intense color corresponds to multibeam data recorded during the campaign ATACAMES (MICHAUD *et al.* 2013). *Less intense color* = older multibeam data from MICHAUD *et al.* (2006); *less intense color* = area without multibeam; *thin black lines* = ship track during the ATACAMES cruise; *black circles with number* = location of plume sites; **b** Flare-shaped backscatter feature in echogram at site 1. **c** Seabed backscatter along the Atacames track (location on **a** = *fine black line* ending with arrows) **d** Seismic profile (location on **a** = *white line*)

detail (Fig. 6e), the dome exhibits NW–SE elongated 20 m high bathymetric ridges. On the seismic profile (Fig. 6d) the dome appears located above a large diapir outcropping at the seafloor. To the Northeast, below the platform, the NE–SW trending seismic profile exhibits well-stratified sedimentary unit (a on Fig. 6d) that overlay a deeper unit (b on Fig. 6d), which is highly deformed. These two units are affected by sub-

vertical faults. Next to the fault located furthest to the East (CDP 12500, Fig. 6d), the folded geometry of the reflectors of the upper unit indicates some contraction; meanwhile the vertical offset of the top of deeper unit indicates a normal component. The two plume sites 16 and 17 are located southward on the upper slope (site 16 and 17, Table 1; Fig. 2) of the Gulf of Guayaquil. These plumes are located south of the Guayaquil

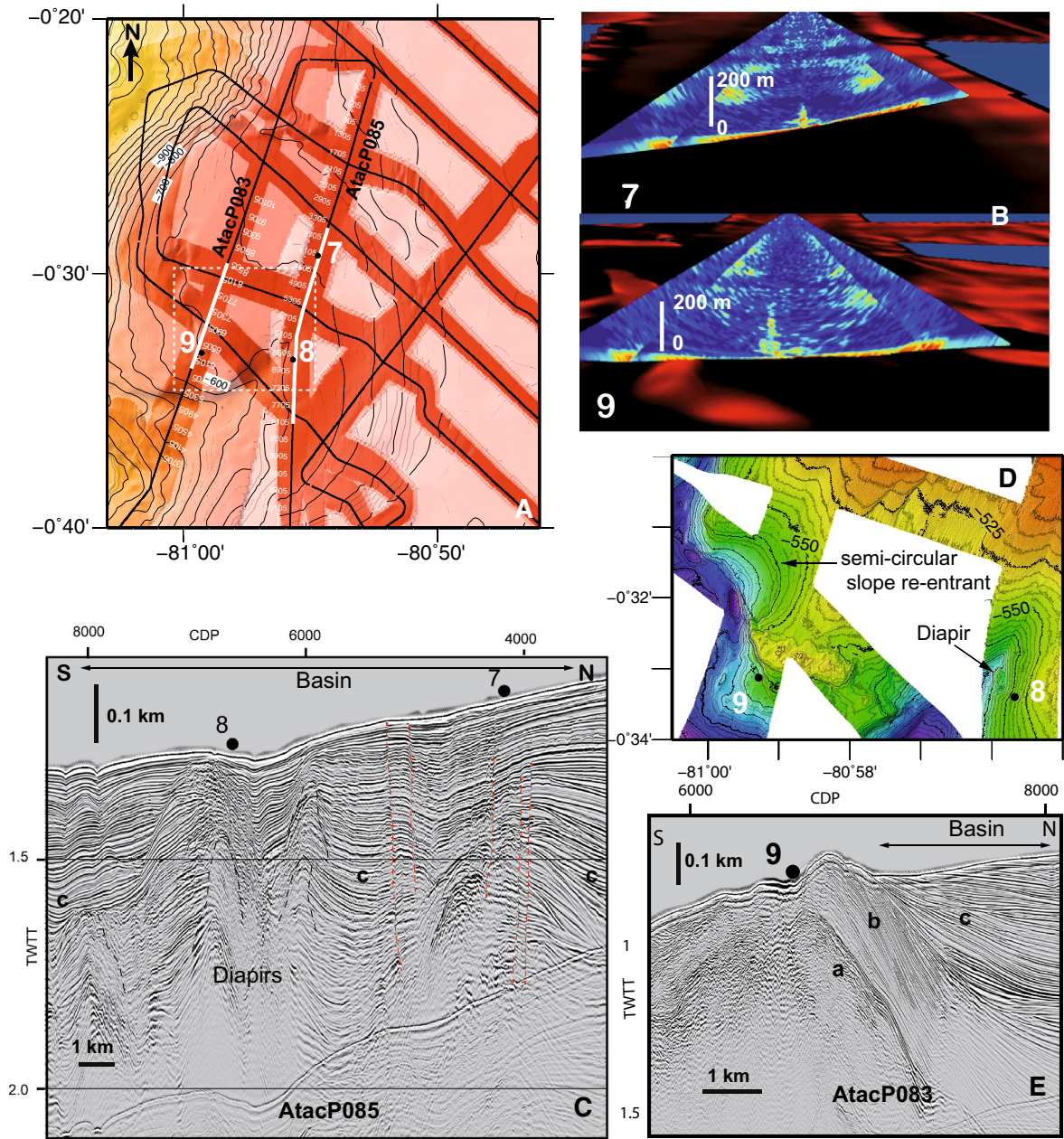


Figure 4

a Bathymetric map with *curves* every 20 m (location on Fig. 2) of the Jama area (grid cell 50 m). *More intense color* corresponds to multibeam data recorded during the campaign ATACAMES (MICAUD *et al.* 2013). *Less intense color* = older multibeam data from MICAUD *et al.* (2006); *less intense color* = area without multibeam. *Thin black lines* = ship track during the ATACAMES cruise. *Thin dotted white line* = location of bathymetric zoom of **d**. **b** Flare-shaped backscatter feature in echogram at site 7 and site 9. **c** Seismic profile in the basin (location **a** = white line). **d** Bathymetric zoom (*curves* every 5 m) of the site 8 and 9 area (grid cell 10 m). **e** Seismic profile crossing the basin southern boundary (location on **a** = white line)

canyon (Fig. 2), which is characterized by an irregular morphology and many landslides (LOAYZA *et al.* 2014). Plume 17 has a height of about 350 m. From the

seabed, it remains in a vertical position for about 250 m, and then the top of the plume is slightly deflected.

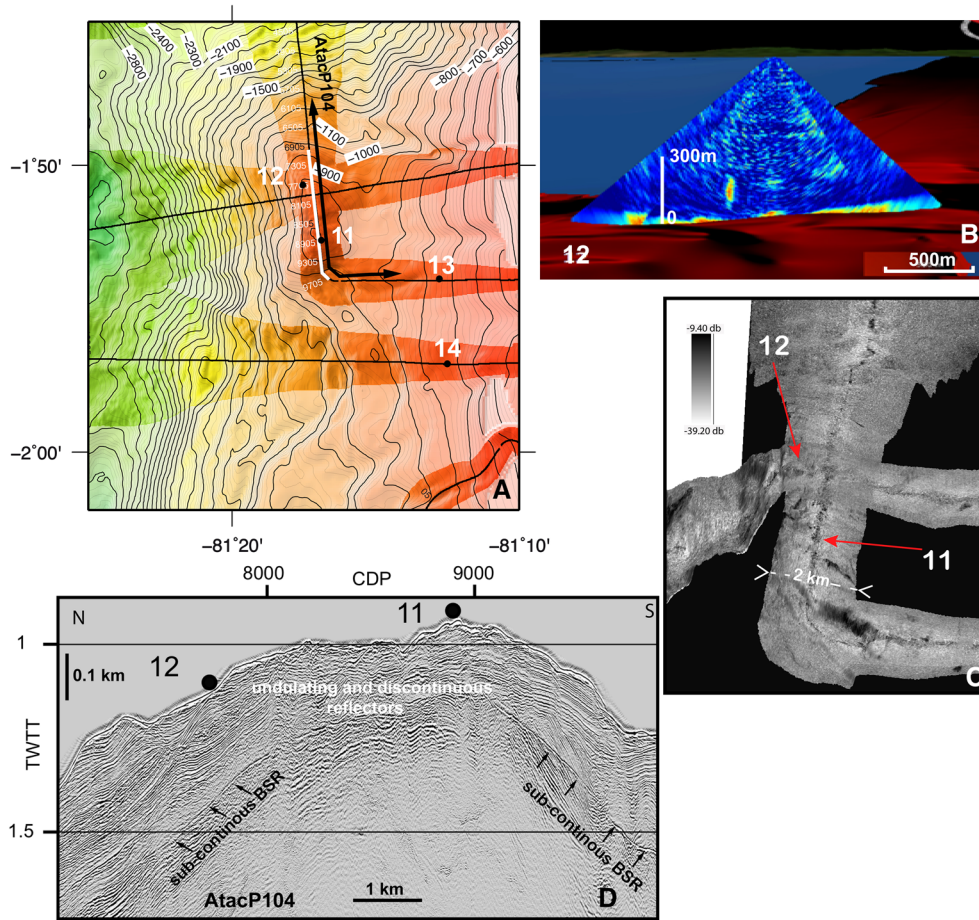


Figure 5

a Bathymetric map with curves every 20 m (location on Fig. 2) of the subducting seamount area (grid cell 50 m). More intense color corresponds to multibeam data recorded during the campaign ATACAMES (MICHAUD *et al.* 2013). Less intense color = older multibeam data from MICHAUD *et al.* (2006); less intense color = area without multibeam. Thin black lines = ship track during the ATACAMES cruise. **b** Flare-shaped backscatter feature in echogram at site 12. **c** Backscatter along the ATACAMES track (location on **a** = fine black line ending with arrows). **d** Seismic profile (location on **a** = white line)

5. Potential Geological Controls

Numerous and various echoes were recorded in the water column during the ATACAMES cruise. They show a high variability in size but they usually form subvertical elongated flares rooted at the seafloor. This geometry of the echoes is typical of gas emissions (OBZHIROV *et al.* 2004; DUPRÉ *et al.* 2014). We interpret the 17 detected acoustic anomalies as the presence of gas bubbles in the water column. Few of them are slightly inclined probably depending on the strength of the mid-water depth current effects. The plume site 1, which is more than 500 m high, is

the most spectacular of the detected sites with probably the highest flow rates. Site 15 that presents several plumes is probably also associated with a significant flow but this needs to be confirmed by in situ measurements,

5.1. Seepage Distribution and Active Tectonics

5.1.1 Faults

Some of the plume sites are clearly related to regional fault systems. Plume site 1 is located just above a highly deformed area (Fig. 3d). The Ancon fault,

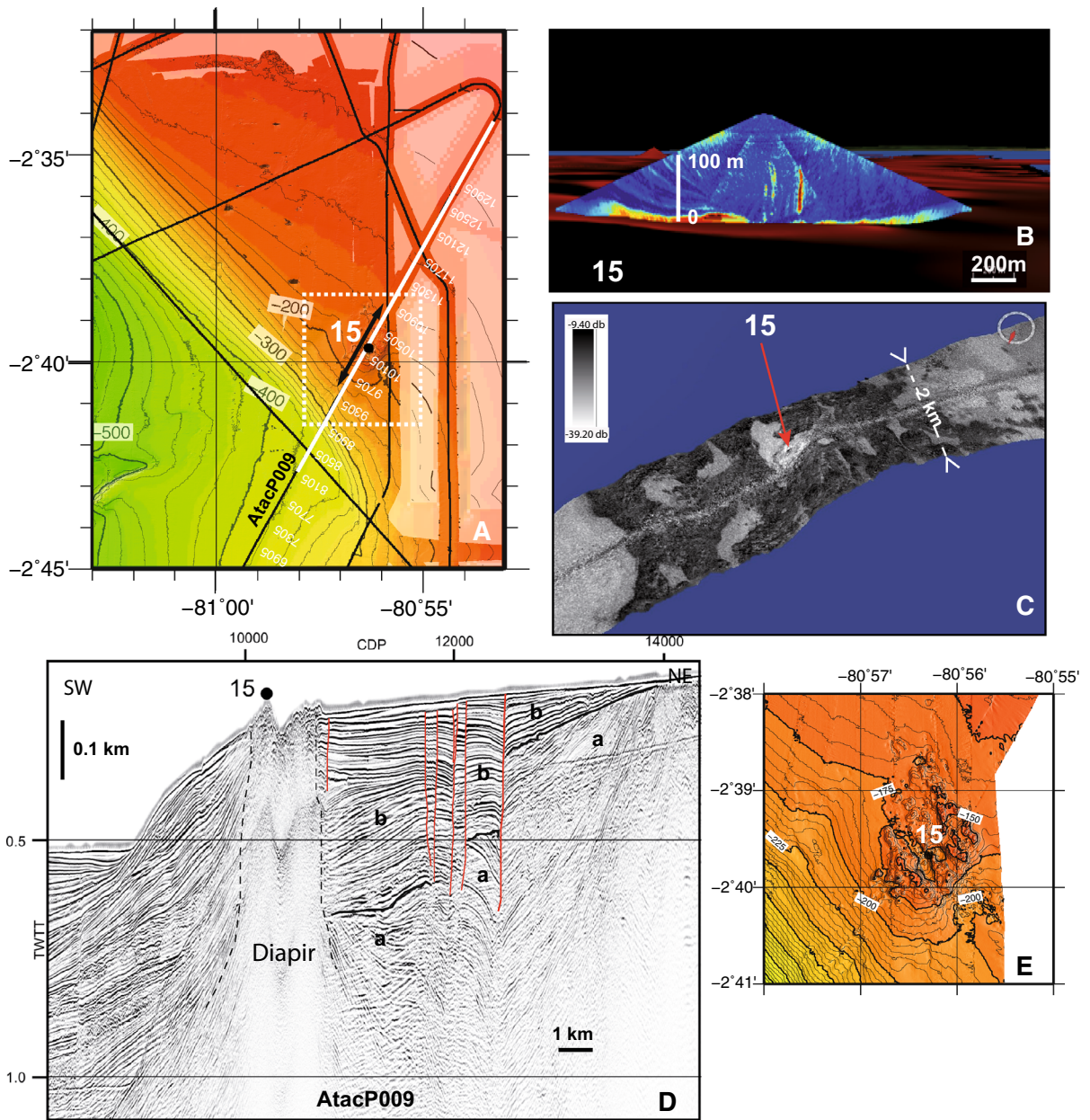


Figure 6

a Bathymetric map with *curves* every 20 m (location on Fig. 2) of the Guayaquil gulf area (grid cell 50 m). *More intense color* corresponds to multibeam data recorded during the campaign ATACAMES (MICHAUD *et al.* 2013). *Less intense color* = older multibeam data from MICHAUD *et al.* (2006) and from PAZMIÑO *et al.* 2010; *less intense color* = area without multibeam. *Thin red lines* = ship track during the ATACAMES cruise. **b** Flare-shaped backscatter feature in echogram at site 15. **c** Backscatter along the ATACAMES track (location **a** = fine black line ending with arrows). **d** Seismic profile (location on **a** = white line). Red lines = faults. **e** Bathymetric zoom (*curves* every 5 m, grid cell 10 m) of the diapir area (location on **a** = white dotted line square)

which is a major regional tectonic structure, is described a few kilometers to the north (COLLOT *et al.* 2004, 2008) but, so far, its southern tip has

remained unclear. We cannot clearly state concerning the origin and causes of the seepage at site 1. Nevertheless, this site is closely associated with a

deformed area. And the Ancon fault activity might be at the origin of these observed deformations.

Plume sites 7, 8, and 9 are detected in the area where the offshore prolongation of the Jama fault system is suggested (COLLOT *et al.* 2004) at the edge of an upper slope sedimentary basin (MICHAUD *et al.* 2015). In contrast to the site 1 area, this area is not characterized by a significant deformation but by small faults rooted in diapirs cutting through the uppermost layers of the sedimentary basin (Fig. 4c). We infer that these small faults act as fluid migration pathways, which seeps on the seafloor at site 7. Site 8 lies on a diapir exposure on the sea bottom (Fig. 4c, d). Site 9 is located at the foot of linear scarp breached by a spoon-shaped reentrant (Fig. 4d, e) interpreted here as the scar of a slope failure. These slope instabilities might have exposed the source rocks and allowed the fluids to escape. Furthermore, this assumed source rocks are tilted and this geometry would perhaps have been able to facilitate the migration of fluids following the layers to escape until the seawater. This assumed source rocks at site 9 probably extend beneath the basin, possibly supplying seepages at sites 7 and 8.

In the gulf of Guayaquil, the zone of fluid expulsion 15 (Fig. 6a) is coincident with a large diapir (Fig. 6d), outcropping at the seafloor in NW–SE 20 m high elongated ridges. Immediately north of the diapir, the sediments of the shelf are affected by vertical dominantly extensional faults (Fig. 6d) showing a complex deformation pattern including some evidence for contraction, which might reflect the surface expression of a transcurrent faulting structure. It is this transcurrent faulting structure that probably shapes the nearby diapir and its topmost-ridged surface. This suggests that NW–SE trending faults parallel to the shelf break control the diapir and the associated plume 15. The root of the diapir is not identified in the seismic line (Fig. 6d), indicating that the under-compacted material below, from which it originates, is located deeper than 1 s TWTT below seafloor. Southward, several mud diapirs were reported along the N-S trending shelf break of the Guayaquil gulf (WITT *et al.* 2006). But on the contrary to the diapir at the site 15, none of them

pierce through the seafloor. A layer of late Pleistocene sediment uncomfortably overlays these diapir structures. This suggests that these diapirs are inactive since the late Pleistocene (WITT *et al.* 2006), whereas our observations suggest that the diapir located at site 15 is still active.

5.1.2 Seamount Subduction

The four plume sites 11, 12, 13, and 14 are grouped in an area where swath-bathymetric data (Figs. 2 and 5a) show the deformation of the surface of the margin above a subducting seamount (SAGE *et al.* 2006; COLLOT *et al.* 2009; SANCLEMENTE 2014). The base of the lower slope is indented (Fig. 2) with a re-entrant. The middle slope exhibits a N-S elongated bulge corresponding to a local uplifted zone (i.e. the supposed position of the subducted seamount), bounded seaward by sedimentary slides. Across this bulge, the seismic profile (Fig. 5d) reveals a zone with undulating and discontinuous reflectors. This zone, located above the supposed position of the subducted seamount, focuses the upward fluid migration at plume sites 11 and probably 12 through the uppermost layers.

5.1.3 Isolated Plumes and No-Plume Zones

No obvious tectonic or slope failure structures underline sites 4, 5, 6, and 10 (Fig. 2). These sites are located on a smooth regular slope bathed at 600 m of water depth. At the latitudes of sites 4, 5, and 6, a large thick Neogene sedimentary basin sits on the upper slope (HERNANDEZ *et al.* 2014). These plumes sites are located on the outer edge of the basin, which could provide the source of fluid seepage. No site was detected around La Plata Island, whereas it is considered as one of the more actively uplifting area of the continental shelf (PEDOJA *et al.* 2006; PROUST *et al.* 2016). Due to the acoustic sampling strategy during ATACAMES cruise, we cannot exclude that the seep area are not fully constrained. However, the reduced sediment thickness around La Plata Island (PROUST *et al.* 2016), might not provide enough fluids to supply seepage at the sea floor.

5.2. Seepage Distribution and BSR

Plume sites 1, 11, and 12 are located above local BSR segments (Figs. 3d and 5d). These BSR-related plume sites are the most spectacular of plume sites recognized along the margin. The first one exhibits the highest plume (500 m high, plume site 1), which may correspond to the highest fluid flow rate. The second one is the area affected by a subducting seamount, which shows the densest occurrence of seeps (four plume sites 11, 12, 13, and 14). Accumulation of gas hydrates corresponding to the BSR should inhibit any migration and associated seabed escapes (JUDD and HOVLAND 2007). Nevertheless, in these two areas, abundant evidences of seabed seepage correlate with deformed and discontinuous reflectors providing pathways for active seeps. We suggest that, active deformation probably disrupts the BSR, which then supplies the plumes. At site 1, close to the Ancon fault, the BSR is partly interrupted as indicated by the seismic profile (Fig. 3d). At site 11 above the subducting seamount (Fig. 5a), the BSR is continuous on both sides of the ridge, while directly below the ridge, it is highly disrupted (Fig. 5d).

6. Conclusions

This paper documents for the first time 17 acoustic flares, interpreted as originating from gas expulsions, on the seafloor of the Ecuadorian margin. Water column acoustic backscatter data acquired during the ATACAMES campaign in 2012 image these flares. From this first, non-exhaustive account of water-column acoustic flares, acoustic anomalies are mainly observed on the upper slope or at the shelf break. Whatever the fluid origin, the spatial distribution of the seeps suggests potential first-order relationship with tectonics and sedimentary features. At regional scale, most seeps follow the deformation structures seen in high-resolution seismic surveys. Further investigation involving full multibeam coverage and dedicated seismic data would help to refine the fluid migration pathways in the sedimentary column and their link to the regional hydrocarbon system.

Acknowledgments

We thank the crew of R/V L'Atalante and GENAVIR. This work was supported by Institut National des Sciences de l'Univers du Centre National de la Recherche Scientifique (INSU). Thanks to Institut de la Recherche et du Développement (IRD), the Laboratoire Mixte International "Séismes et Volcans" (LMI) and to the Instituto Oceanográfico de la Armada (INOCAR). This work was partially sponsored by the Ministry of Higher Education, Science, Technology and Innovation of the Republic of Ecuador (SENESCYT). We thank the anonymous reviewers for their constructive comments, which helped us to improve the manuscript.

REFERENCES

- BOURGOIS J (2013) *A review on tectonic record of strain buildup and stress release across the andean forearc along the gulf of guayaquil-tumbes basin (GGTB) near ecuador-peru border.* Intern Journ Geosc 4:618–635. doi:10.4236/ijg.2013.43057.
- COLLOT J-Y, MARCAILLOU B, SAGE F, MICHAUD F, AGUDELO W, CHARVIS P, GRAINDORGE D, GUTSCHER MA, SPENCE G (2004) *Are rupture zone limits of great subduction earthquakes controlled by upper plate structures? Evidence from MCS data acquired across the N-Ecuador-SW Colombia margin.* J Geophys Res 109:B11103. doi:10.1029/2004JB003060.
- COLLOT J-Y, MIGEON S, SPENCE G, LEGONIDEC Y, MARCAILLOU B, SCHNEIDER, J-L, MICHAUD, F, ALVARADO, A, LEBRUN, J-F, SOSSON, M, PAZMIÑO, A, 2005. *Seafloor margin map helps in understanding subduction earthquakes.* EOS Transactions, American Geophysical Union, 86(46): 464–466.
- COLLOT J-Y, AGUDELO W, RIBODETTI A, MARCAILLOU B (2008) *Origin of a crustal splay fault and its relation to the seismogenic zone and underplating at the erosional north Ecuador–south Colombia oceanic margin.* J Geophys Res 113:B12102. doi:10.1029/2008JB005691.
- COLLOT J-Y, MICHAUD F, ALVARADO A, MARCAILLOU B, SOSSON M, RATZOV G, MIGEON S, CALAHORRANO A, PAZMIÑO A (2009) *Visión general de la morfología submarina del margen convergente de Ecuador- Sur de Colombia: implicaciones sobre la transferencia de masa y la edad de la subducción de la Cordillera de Carnegie.* In: COLLOT JY, SALLARES V, PAZMIÑO A (ed) *Geología y Geofísica Marina y Terrestre del Ecuador.* Publicacion CNDM-INOCAR-IRD, PSE001-09, Guayaquil, Ecuador, pp. 47–74.
- DANO A, MIGEON S, PRAEG D, CERAMICOLA S, AUGUSTIN JM, KETZER JM, AUGUSTIN AH, DUCASSOU E, MASCLE J, (2014) *Fluid Seepage in Relation to Seabed Deformation on the Central Nile Deep-Sea Fan, Part 1: Evidence from Sidescan Sonar Data S.* KRSTEL et al. (eds.), *Submarine Mass Movements and Their Consequences*, Advances 129 in Natural and Technological Hazards Research 37, DOI 10.1007/978-3-319-00972-8 12:129–139 .

- DENIAUD Y, BABY P, BASILE C, ORDOÑEZ M, MONTENEGRO G, MASCLE G (1999) *Ouverture et évolution tectono-sédimentaire du Golfe de Guayaquil: bassin d'avant-arc néogène et quaternaire du Sud des Andes équatoriennes*. C. R. Acad. Sci. Paris, 328: 181–187.
- DEYNOUX M, PROUST JN, DURAND J, MERINO E (1990) *Water transfer cylindrical structures in the Late Proterozoic eolian sandstones in the Taoudeni Basin, West Africa*. Sedim. Geol., 66:227–242.
- DOMINGUEZ S, LALLEMAND S, MALAVIEILLE J, VON HUENE R (1998) *Upper plate deformations associated with seamount subduction*, Tectonophysics, 293: 207–224.
- DUPRÉ S, WOODSIDE J, KLAUCKE I, MASCLE J, FOUCHER J-P (2010) *Widespread active seepage activity on the Nile Deep Sea Fan (offshore Egypt) revealed by high-definition geophysical imagery*. Marine Geology, 275(1–4), 1–19.
- DUPRÉ S, BERGER L, LE BOUFFANT N, SCALABRIN C, BOURILLET J-F (2014) *Fluid emissions at the Aquitaine Shelf (Bay of Biscay, France): A biogenic origin or the expression of hydrocarbon leakage?* Continental Shelf Research, 88, 24–33.
- DUPRÉ S, SCALABRIN C, GRALL C, AUGUSTIN J-M, HENRY P, SENGÖR AMC, GÖRÜR N, ÇAGATAY MN, GÉLI L (2015) *Tectonic and sedimentary controls on widespread gas emissions in the Sea of Marmara: Results from systematic, shipborne multibeam echo sounder water column imaging*, J. Geophys. Res. Solid Earth, 120, doi:10.1002/2014JB011617.
- EGUEZ A, ALVARADO A, YEPES H, MACHETTE M, COSTA C, DART R (2003) *Database and map of Quaternary faults and folds of Ecuador and its offshore regions*. US Geological Survey, Open File Rep. 03–289.
- GAY A, LOPEZ M, BERNDT C, SÉRANNE M, (2007) *Geological controls on focused fluid flow associated with seafloor seeps in the Lower Congo Basin*, Marine Geology 244; 68–92.
- GÉLI L, HENRY P, ZITTER T, DUPRE S, TRYON M, CAGATAY M, DE LEPINAY B, LE PICHON X, SENGOR A, GORUR N, NATALIN B, UCARKUS G, OEZEREN S, VOLKER D, GASPERINI L, BURNARD P, BOURLANGÉ S (2008). *Gas emissions and active tectonics within the submerged section of the North Anatolian Fault zone in the Sea of Marmara*. Earth and Planetary Science Letters, 274(1–2): 34–39.
- GERMAN CR, PARSON LM, MILLS RA (1996) *Mid-ocean ridges and hydrothermal activity*. In: Oceanography. An Illustrated Guide. C.P. SUMMERHAYES and S.A. THORPE, eds, p. 152–164.
- GRAINDORGE D, CALAHORRANO A, CHARVIS P, COLLOT J-Y, BETHOUX N (2004) *Deep structures of the margin and the Carnegie Ridge, possible consequence on great earthquake recurrence interval*. Geoph Res Lett 31. doi:10.1029/2003GL018803.
- GREINERT, J, ARTEMOV, Y, EGOROV, V, DE BATIST, M, MCGINNIS, D, (2006) *1300-m-high rising bubbles from mud volcanoes at 2080 m in the Black Sea: Hydroacoustic characteristics and temporal variability*. Earth and Planetary Science Letters 244:1–15. doi:10.1016/j.epsl.2006.02.011.
- GUTSCHER M-A, MALAVIEILLE J, LALLEMAND S, COLLOT J-Y (1999) *Tectonic segmentation of the North Andean margin: impact of the Carnegie ridge collision*. Earth and Planetary Science Letters 168:255–270.
- HERNÁNDEZ M-J, MICHAUD F., COLLOT J-Y, PROUST J-N, ORTEGA R., ALEMÁN A-M (2014) *The Neogene Forearc Basins of the Ecuadorian Shelf (1°N-2°S): Preliminary Interpretation of a Dense Grid of Mcs Data* Abstract T11C-4578 presented at 2014 Fall Meeting, AGU, San Francisco, Calif., 15–19 Dec.
- HORNAFIUS JS, QUIGLEY D, LUYENDYK BP (1999) *The world's most spectacular marine hydrocarbon seeps (Coal Oil Point, Santa Barbara Channel, California): Quantification of emissions*. Journal of Geophysical Research 104. doi: 10.1029/1999JC900148.
- JUDD AG, HOVLAND, M (2007) *Seabed Fluid Flow. The Impact on Geology, Biology and the Marine Environment*. Cambridge University Press, Cambridge.
- KRABBEHÖFT A, NETZEBAND G, BIALAS J, PAPPENBERG C (2010) *Episodic methane concentrations at seep sites on the upper slope Opouawe Bank, southern Hikurangi Margin, New Zealand*, Marine Geology, 272 (1/4):71–78. DOI 10.1016/j.margeo.2009.08.001.
- LOAYZA G, PROUST J-N, MICHAUD F, COLLOT J-Y (2014), *Evolution pléistocène du système de canyons du golfe de Guayaquil (Equateur)*. Contrôles paléo-climatique et tectonique, 14^{ème} ASF congrès, Paris, page 248.
- LONCKE L., MASCLE J., and FANIL SCIENTIFIC PARTIES, (2004) *Mud volcanoes, gas chimneys, pockmarks and mounds in the Nile deep-sea fan (Eastern Mediterranean): geophysical evidences*, Marine and Petroleum Geology 21,6: 669–689.
- MARCAILLOU, B, SPENCE G, COLLOT J-Y, WANG K (2006) *Thermal regime from bottom simulating reflectors along the north Ecuador–south Colombia margin: Relation to margin segmentation and great subduction earthquakes*, Journal Geophysiscal Research 111, B12407, doi:10.1029/2005JB004239.
- MARCAILLOU B, COLLOT J-Y., RIBODETTI A, D'ACREMONT E, MAHAMAT AA, ALVARADO A (2016) *Seamount subduction at the North-Ecuadorian convergent margin: Effects on structures, inter-seismic coupling and seismogenesis*, Earth and Planetary Science Letters 433, 1 January 2016, Pages 146–158.
- MASCLE J, FLORE M, PRAEG D, BROSOLO L, CAMERA L, CERAMICOLA S, DUPRE S (2014) *Distribution and geological control of mud volcanoes and other fluid/free gas seepage features in the Mediterranean Sea and nearby Gulf of Cadiz*. Geo-marine Letters, 34(2–3), 89–110. <http://dx.doi.org/10.1007/s00367-014-0356-4>.
- MICHAUD F, COLLOT J-Y, ALVARADO A, Lopez E y el personal científico y técnico del INOCAR. (2006) Republica del Ecuador, Batimetría y Relieve Continental, publicación IOA-CVM-02-Post. INOCAR, Guayaquil.
- MICHAUD F, WITT C, ROYER J-Y (2009) *Influence of the Carnegie ridge subduction on Ecuadorian geology: reality and fiction*: In: KAY S, RAMOS V, and DICKINSON WR (eds) *Backbone of the Americas: Shallow Subduction, Plateau Uplift and Ridge and terrane Collision*. *Geol Soc Am Memoir* 204:217–228 doi:10.1130/2009.1204.10.
- MICHAUD F, PROUST J-N, COLLOT J-Y, the ATACAMES scientific team (2013) *Sediments distribution and tectonic faults (Ecuadorian shelf): preliminary results of the ATACAMES Cruise (2012)*, Abstract T23B-06 presented at 2013 Meeting of the Americas, AGU, Cancun, Mexico, 14-17 May.
- MICHAUD F, PROUST J-N, COLLOT J-Y, LEBRUN J-F, WITT C, RATZOV G, POUDEIROUX H, MARTILLO C, HERNÁNDEZ M-J, LOAYZA G, PENAFIEL L, SCHENINI L, DANO A, GONZALEZ M, BARBA D, DE MIN L, PONCE ADAMS G, URRESTA A, CALDERON M, (2015) *Quaternary sedimentation and active faulting along the Ecuadorian shelf: preliminary results of the ATACAMES Cruise (2012)*, Marine Geophysical Research, 36, 1:81–98.
- MEREWETHER R, OLSSON M-S, LONSDALE P (1985) *Acoustically detected hydrocarbon plumes rising from 2-km depths in*

- Guaymas Basin, Gulf of California* *J. Geophys. Res.*, 90 (1985), pp. 3075–3085.
- NOCQUET J-M, MOTHES P, ALVARADO A (2009) Geodesy, geodynamics and earthquake cycle in Ecuador. Geology and marine and onland Geophysics of Ecuador: from the continental coast to the Galapagos Islands. In COLLOT JY, SALLARES V, PAZMIÑO A (eds) *Geología y Geofísica Marina y Terrestre del Ecuador*. Publicación CNDM-INOCAR-IRD, PSE001-09, Guayaquil, Ecuador pp 83–94.
- NOCQUET J-M, VILLEGAS-LANZA JC, CHLIEH M, MOTHES PA, ROLANDONE F, JARRIN P, CISNEROS D, ALVARADO A, AUDIN L, BONDOUX F, MARTIN X, FONT Y, RÉGNIER M, VALLÉE M, TRAN T, BEAUVAL C, MAGUIÑA MENDOZA JM, MARTINEZ W, TAVERA H, YEPES H, (2014) *Motion of continental slivers and creeping subduction in the northern Andes*, *Nature Geosciences*, 7 (4) (2014), pp. 287–291. <http://dx.doi.org/10.1038/ngeo2099>
- OBZHIROV A, SHAKIROV R, SALYUK A, SUESS E, BIEBOW N, SALOMATIN A (2004) *Relations between methane venting, geological structure and seismo-tectonics in the okhotsk sea*, *Geo-marine letters*, 24:135–139.
- PAULL CK, BOROWSKI WS, RODRIGUES N M, (1998) ODP Leg 164 Shipboard Scientific Party, Marine Gas Hydrate Inventory: Preliminary Results of ODP Leg 164 and Implications for Gas Venting and Slumping Associated with the Blake Ridge Gas Hydrate Field. In: HENRIENT, J. P., MIENERT, J., eds., *Gas Hydrates: Relevance to World Margin Stability and Climate Change*. *Geol. Soc. London Spec. Publ.*, 137: 153–160.
- PAZMIÑO A, ZAPATA C, MICHAUD F, MARTILLO C, LOAYZA G (2010) Reporte Científico a Bordo del B.I.- 91 “Orion” Estudio Geológico del Margen de Plataforma Continental del Golfo de Guayaquil (GEMAC- 1), Diciembre 2010.
- PEDOJA K, DUMONT JF, LAMOTHE M, ORTLIEB L, COLLOT JY, GHALEB B, AUCLAIR M, ALVAREZ V, LABROUSSE B (2006) *Plio-quaternary uplift of the manta peninsula and La Plata Island and the subduction of the Carnegie Ridge, central coast of Ecuador*. *J S Am Earth Sci* 22:1–21.
- PRAEG D, KETZER JM, AUGUSTIN AH, MIGEON S, CERAMICOLA S, DANO A, DUCASSOU E, DUPRE S, MASCLE J, RODRIGUES LF (2014) *Fluid seepage in relation to seabed deformation on the central Nile Deep-Sea Fan, part 2: evidence from multibeam and sidescan imagery*. *Advances in Natural and Technological Hazards Research*, 37, 141–150.
- PROUST J-N, MARTILLO C, MICHAUD F, COLLOT J-Y, DAUTEUIL O (2016) *Subduction of seafloor asperities revealed by detailed stratigraphic analysis of the active margin shelf sediments of Central Ecuador*. *Marine Geology (in press)*.
- RANERO CR, VON HUENE R (2000) *Subduction erosion along the Middle America convergent margin*: *Nature*, v. 404, p. 335–357.
- REYES P, MICHAUD F (2012) Mapa Geológico de la Margen Costera Ecuatoriana (1500000) EPPetroEcuador-IRD (eds), Quito Ecuador.
- RÖMER M, SAHLING H, PAPE Th, DOS SANTOS FERREIRA C, WENZHÖFER F, BOETIUS A, BOHRMANN G, (2014) *Methane fluxes and carbonate deposits at a cold seep area of the Central Nile Deep Sea Fan, Eastern Mediterranean Sea*, *Marine Geology*, 347: 27–42.
- SANCLLEMENTE E (2014) Seismic imaging of the structure of the central Ecuador convergent margin: relationship with the inter-seismic coupling variations, *Earth Sciences*. Thèse Université de Nice-Sophia Antipolis 2014.
- SAGE F, COLLOT J-Y, RANERO CR (2006) *Interplate patchiness and subduction-erosion mechanisms: Evidence from depth-migrated seismic images at the central Ecuador convergent margin*, *Geology*, v. 34; no. 12; pp. 997–1000; doi: [10.1130/G22790A.1](https://doi.org/10.1130/G22790A.1).
- SCHNEIDER VON DEIMLING J, BROCKHOFF J, GREINERT J (2007) *Flare imaging with multibeam systems: Data processing for bubble detection at seeps*, *Geochem. Geophys. Geosyst.*, 8, Q06004, doi:[10.1029/2007GC001577](https://doi.org/10.1029/2007GC001577).
- SUESS E, TORRES L, M.E., BOHRMANN G, COLLIER RW, GREINERT J, LINKE P, REHDER G, Trehu A, Wallmann K, Winckler G, Zuleger E, (1999) Gas hydrate destabilization: enhanced dewatering, benthic material turnover and large methane plumes at the Cascadia convergent margin, *Earth and Planetary Science Letters* 170 (1999) 1–15.
- WITT C, BOURGOIS J, MICHAUD F, ORDOÑEZ M, JIMENEZ N, SOSSON M (2006) *Development of the Gulf of Guayaquil (Ecuador) as an effect of the North Andean Block tectonic escape since the lower Pleistocene*. *Tectonics* 25. doi:[10.1029/2004TC001723](https://doi.org/10.1029/2004TC001723).

(Received July 2, 2015, revised December 18, 2015, accepted December 20, 2015)